

**THIRTEENTH MEETING OF THE UJNR
PANEL ON FIRE RESEARCH AND SAFETY,
MARCH 13-20, 1996**

VOLUME 2

Kellie Ann Beall, Editor

June 1997
Building and Fire Research Laboratory
National Institute of Standards and Technology
Gaithersburg, MD 20899



U.S. Department of Commerce
William M. Daley, *Secretary*
Technology Administration
Gary R. Buchula, *Acting Under Secretary for Technology*
National Institute of Standards and Technology
Robert E. Hebner, *Acting Director*

RADIATION PROPERTIES AND FLAME STRUCTURE OF LARGE HYDROCARBON POOL FIRES

Hiroshi Koseki

Fire Research Institute
3-14-1 Nakahara Mitaka, Tokyo 181 Japan

ABSTRACT

In order to understand properties of large tank fires and flame structure, external radiation was measured in several size pan fire experiments. In the large fires, radiation was blocked by a huge amount of smoke around the flame, and most of the radiation was emitted from flame base. In order to explain this result other flame properties, smoke emission, flame temperature, gas velocity and gas concentration in the flame, and the burning rate were also measured. Discussion of the radiation and flame structure is presented base on these data. It is found that most combustion was completed in the low part of flame, and gas flow in the radial direction in the upper part of flame played an important role in emitting smoke.

1. INTRODUCTION

In fire fighting and fire safety design of oil tanks, it is very important to understand radiation properties of large tank fires, and it is well known that external radiation is blocked by huge amount of smoke produced around the flame in large tank fires. This is known as the 'smoke blockage effect'. To clarify this phenomenon, external radiation has been measured during FRI large scale pool fire experiments at FRI [for example, 1,2,3,4]. Other flame properties, flame temperature, and burning rate were also measured to understand flame structure by FRI, NIST and others [For example, 9,10]. Currently smoke emission has been measured by Evans, Walton and Mulholland at NIST [5,6,7,8]. With these smoke data global study on radiation properties and flame structure of large tank fires have been performed.

2. EXPERIMENTAL

A series of experiments were conducted through collaboration between BFRL of NIST, USA and FRI, Japan including a 15 m square pan fire test using crude oil at the test facilities of the US Coast Guard in the Mobile, AL. Table 1 is a listing of experiments using crude oil, that is, pan diameter, fuel and test facilities. Most tests were done using the NIST large calorimeter and the FRI large test facility. Figure 1 shows a schematic of the 2.7 m square pan test, which was done inside the FRI test facilities. For getting local radiant emittance of the crude oil flame, an IR-camera, Nippon Avionics TVS-2000ST was used. Its specifications are shown in Table 2. The steps in the processing of the IR-camera data reduction are shown in Figure 2. Temperature data obtained with the IR-camera were converted into radiation information by Stefan-Boltzmann's law using a Black-body calibrator. In order to obtain local radiant emittance of flames, slit-attached radiometers were used in the heptane fire test. Using slit-attached radiometers, we can divide the flame into four or five parts vertically at the maximum, the IR-camera gave 10 to 30 slices of the flame easily. Other measurements relating burning rate, gas velocity, temperature, gas concentration were also performed in the tests except for the 15 m square pan test. Details of measurements are shown previous papers [1,2]. In the 15 m square pan fire test, the burning rate was measured. In the tests crude oil, popular light crude oil, Arabianlight crude oil, Murban crude oil

and Louisiana crude oil were used.

3. RESULTS AND DISCUSSION

In order to obtain scale dependency on pan diameter, previous data [1,2,3] and FRI large test data [4] were also added into the discussion of the measurements.

3.1 Total irradiance

Total irradiance from the whole flame to a target far from flame was measured with wide-angle radiometers and an IR-camera. Figure 3 shows difference between irradiances at $L/D=7.1$ measured by both instruments in the 15 m square pan fire test. Here L is a distance between flame axis and a target. D is an effective pan diameter, the diameter of circular which the same area as the pool fire as vessel, here $D=17.2$ m. In the first few minutes from ignition, both data are in very good agreement, but during the steady state burning the difference was a maximum of about 30 %. The difference maybe due to differences in the field of view and the time response of the instruments.

Figure 4 shows that irradiance at $L/D=5$ from various size heptane, kerosene and crude oil fires. Data from Refs. [1,2,3,4,11] are added. Around $D<3$ m, average irradiance increased with increasing pan diameter due to emissivity increasing. At $D \doteq 3$ m, emissivity of the flame equals to 1, and radiant emittance was the maximum, then decreased with pan diameter. This decrease maybe due to so-called smoke blockage effect. Smoke were seen around the flame.

3.2 Local radiant emittance

The local radiant emittance of heptane and crude oil fires were measured by wide-angle radiometers and IR-camera. The data are shown in Figure 5 (crude oil) and Figure 6 (heptane). Here the horizontal axis is dimensionless height, H/H_f . Where H is a height from fuel surface and H_f is the average flame height obtained by IR-camera or video camera.

The 2.7 m square crude oil pan fire gave the maximum radiant emittance. The peak of irradiance was at $H/H_f=0.1 \sim 0.2$. Most of the radiation was emitted from flame base. For example about 75 % of total radiation was emitted from the flame base ($0 < H/H_f < 0.4$) in the crude oil 15 m pan fire. The maximum radiant emittance was only 35 kW/m² at $H/H_f=0.08$ and about 120 kW/m² at $H/H_f=0.12$ in 2.7 m square pan fire. A kind of fireball appeared through the black smoke at about $H/H_f=0.8$, regularly, but it did not make a large contribution for average external radiation.

In the heptane fire, the tendency was similar to crude oil fire. The highest local radiant emittance was 220 kW/m² at $H/H_f=0.3$ in the 2.7 m square pan fire. The height of peak local radiant emittance was slightly higher than that of crude oil fire, but most radiation was emitted from the continuous flame zone.

3.3 Smoke emission, pulsation of flame height, isotherms, gas and air flow inside the flame, and gas concentration in the flame

In order to understand the above radiation results, other data which were obtained during the experimentals will be discussed.

(1) Smoke emission

It is believed that smoke emission from flame blocked external radiation. Therefore the relationship between smoke emission and radiation is important

and will be discussed here. As a smoke emission parameter, the dimensionless smoke produce rate, smoke yield (mass smoke production / mass burning rate) as defined by Mulholland et al. [6], was adopted here. Scale dependency of smoke emission has been reported by Mulholland et al. [6,7,8]. External radiation and smoke yield increased with pan diameter until $D=3$ m. Over $D>3$ m, smoke yield may not increase with increasing pan diameter but irradiance at $L/D=5$ decreased drastically (Figure 3). Therefore smoke yield does not seem to directly to radiation decrease in the large scale fires.

Mulholland et al. [8] also measured smoke particle size and found that the primary particle size changed with pan diameter. Primary particle size is related to the resident time of smoke in the flame. When smoke is emitted at a lower height than the flame tip, the resident time would be shorter and the primary particle size would be smaller, so its distribution would be larger. In a large fire, primary particle size and diameter distribution became larger. The results of average diameter and diameter distribution changed from 1 m pan fire to 2.7 m square pan fire. That is, smoke production mode might be change at about $D=2$ m. Visual observations are that, most smoke was seen above flame tip in 1 m pan fire and in the upper part of flame in 2.7 m square pan fire. Therefore in fires larger than about 2 m diameter, smoke is emitted from flame tip and upper part of flame is present around most of the flame surface, and blocks radiation emissions.

(2) Pulsation of flame height

Average flame height was obtained using a video camera, 35 mm camera or IR-camera. The flame height changed regularly. Figure 7 shows the pulsation of flame height obtained with the IR-camera in the heptane 0.60 m pan fire. Following McCaffrey's definition [9], the flame can be divided into the continuous zone and the intermittent zone. The continuous zone height $H_{f(contin.)}$ is about 65 % of average flame height H_f . In large fire, $H_{f(contin.)}$ is 70 ~ 90 % of H_f , but it is difficult to determine this ratio due to smoke existence around upper part of flame. Calculation by Heskettad's equation gave good agreement with the test result for the intermittent flame height [10] which was 20 ~ 40 % larger than average flame height, H_f . It is easy to guess from flame pulsation that radiation from continuous flame zone is much larger than intermittent flame zone, which was the result of the measurement of local radiant emittance.

(3) Isotherms

Figure 8 shows the temperature inside the 6 m heptane flame, which was obtained using about 60 thermocouples. It is found that there is a high temperature ridge from the pan edge to the flame center which means air flow along this zone strongly. The highest temperature zone existed about the height of $H/H_f=0.3$ at the fire axis. It is guessed that below this ridge there existed fuel vapor, and above this ridge there existed burned gases. Figure 9 shows the temperature distribution along the flame axis for several size flames. Flame temperature increased with pan diameter. Huge pan fire data implied this results continuation to 50 m pan fire test, that is, 1380 °C in 30 m and 50 m kerosene fire [11]. Therefore we understand temperature inside the large flame is higher than small flame, but external radiation is smaller due to the smoke around the flame larger than 3 m in diameter.

(4) Gas flow and air flow

Horizontal gas and air flows were obtained. Air entrainment from the flame base to flame tip was more than five times as much as the calculation from the fuel burning data [1,2].

Figure 10 shows the horizontal flow above the 0.3 m heptane pan fire. It was measured along the pan edge vertically using bi-directional tube.

$0 < H/H_f < 0.6$ (\doteq continuous flame zone), it is mostly steady flow, $0.6 < H/H_f < 1.2$ (\doteq intermittent flame zone) flow from the flame to outside were sometimes observed, and $H/H_f > 1.2$ (\doteq plume zone) steady flow were observed again. The horizontal flow observed at the height of $0.6 < H/H_f < 1.20$ played an important role of smoke growth and transportation from inside the flame to the around the flame. This flow must be stronger in larger pan fire, and carries smoke to outside of flame.

(5) Gas concentration

Gas concentration along with the flame axis in several size heptane fires were measured. In order to understand combustion in the flame, dimensionless CO_2 , CO_2^* , was defined [1,2]. That is, $CO_2^* = C_{CO_2} / (C_{CO_2} + C_{CO} + C_{H_2O} + \sum C_{C_mH_n})$. When $CO_2^* = 0.681$ in heptane fire, the combustion must be completed. Figure 11 shows the results using heptane. About $H/H_f = 0.3$, CO_2^* was equal to $0.55 \sim 0.60$, therefore most combustion is finished and most of the heat of combustion was produced below the height of $H/H_f = 0.3$. Therefore the lower part of the continuous flame zone, $H/H_f \leq 0.3$, is the most important region for combustion and radiative heat release.

3.4 Flame structure

With the above data, it is understood that most air flow penetrate into the flame base and most combustion is finished and most of the heat of combustion is produced below the height of $H/H_f = 0.3$. Then a part of reacted gas is emitted from intermittent flame zone, $H/H_f = 0.6 \sim 1.2$. This flow may be stronger in larger pan fires, and may be important in the reacted gas emission. Smoke is emitted along with the reacted gas. Therefore 'Smoke blockage' was predominant in 15 m square pan fire though the smoke yield might not change drastically from 2.7 m square pan to 15 m square pan.

4. CONCLUSIONS

Total and local radiant emittances of hydrocarbon pool fires were measured. 'Smoke blockage' was explained with data of several size heptane and crude oil fires, up to a 15 m square pan. In the large pan fires, a huge amount of smoke existed around the flame, and only flame base, $H/H_f < 0.3$, could be seen. This is the reason that most radiation is emitted from flame base of large fires. Data on gas and air flow, isotherms and gas concentration were in good agreement with radiation results. That is, most combustion was completed lower than $H/H_f = 0.3$.

5. Acknowledgements

The author wishes to acknowledge the cooperation with Drs. David Evans and William D. Walton at NIST in conducting experiments in Japan and in the U.S. The largest test was conducted at the US Coast Guard Test Facility in Mobile, AL, so author also thanks the US Coast Guard for conducting experiment and their help.

References

- 1) Yumoto, T. and Koseki, H., FRI Report 59, p.1 (1985) (in Japanese)
- 2) Koseki, H. and Yumoto, T., Fire Technology 24(1) p.33 (1988)
- 3) Koseki, H. and Yumoto, T., Fire Safety Science 2 p.231 (1988)
- 4) FRI Technical Report No.8 (1976) (in Japanese)
- 5) Evans, D. et al, Proceeding of 15th AMOP Technical seminar p.593 (1992)
- 6) Mulholland et al., Fire Safety Science 2 p.347 (1989)
- 7) Koseki, H. and Mulholland, Fire Technology 27(1) p.54 (1991)
- 8) Mulholland et al, Proceedings of 13 th UJNR Meeting (March 1996)

- 9) McCaffrey, B., NBS-IR 79-1910 (1979)
- 10) Heskestad, G., Fire Safety Journal 5, p.103 (1983)
- 11) JASE, Oil Tank Fire Test (1981) (in Japanese)

Table 1 Outline of experimental using crude oil

Pan Diameter	Place	Fuel
0.4 m	NIST	Arabian Louisiana
0.6 m	NIST	
1.0 m	FRI	
2.7 × 2.7 m	FRI	
15 × 15 m	Mobile	Louisiana

Table 2 Speculations of IR-camera

Type, Manufacture	TVS 2000ST, Nippon Avionics Co. Ltd.
Detector	In-Sb
Spectral Range	3.0 to 5.4 μ m
Focus Range	254 mm to ∞
Time constant	< 1 μ s
Spatial resolution	2.18 m rad

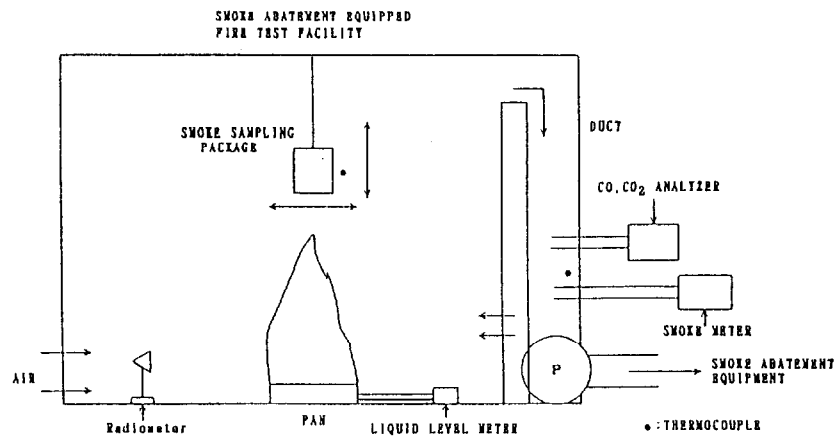


Figure 1 Schematic illustration of the experiment at FRI large test facilities maximum experiment is effective pan diameter=3 m

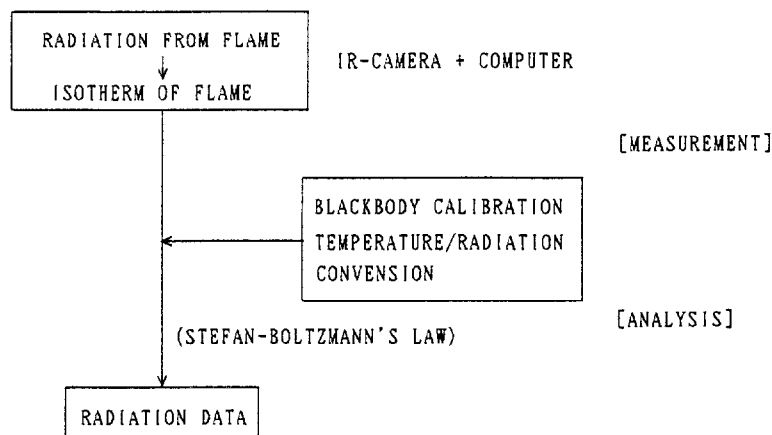


Figure 2 Process of IR-camera data reduction

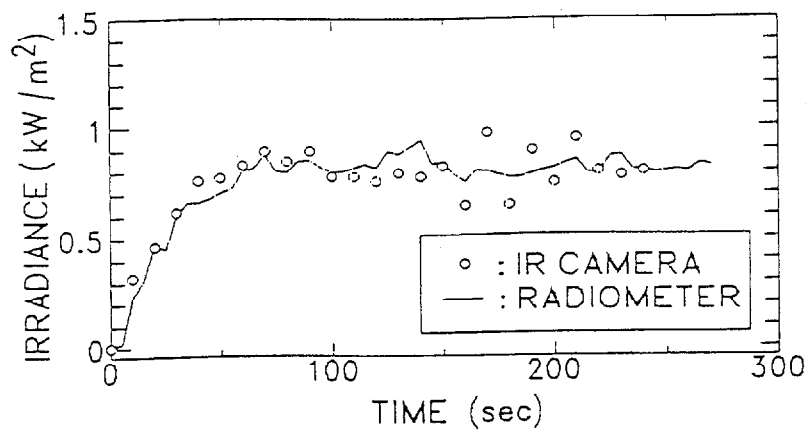


Figure 3 Comparison of time history of irradiance by IR-camera and wide angle radiometer Equipments were set at L/D=7.1

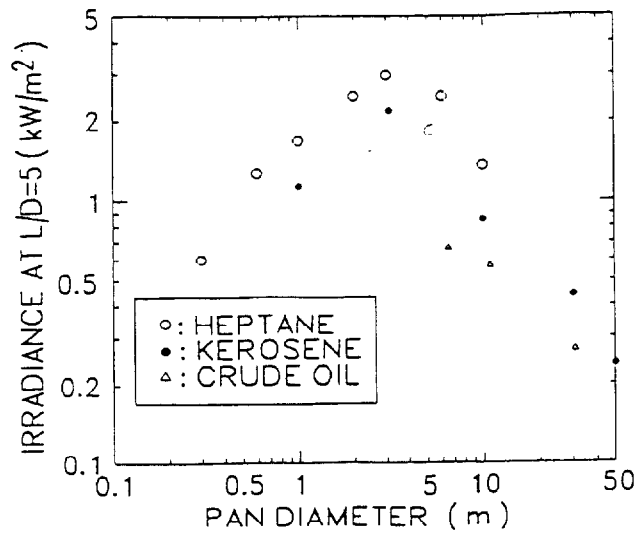


Figure 4 Scale dependency of irradiance at $L/D=5$ for heptane, kerosene and crude oil fires

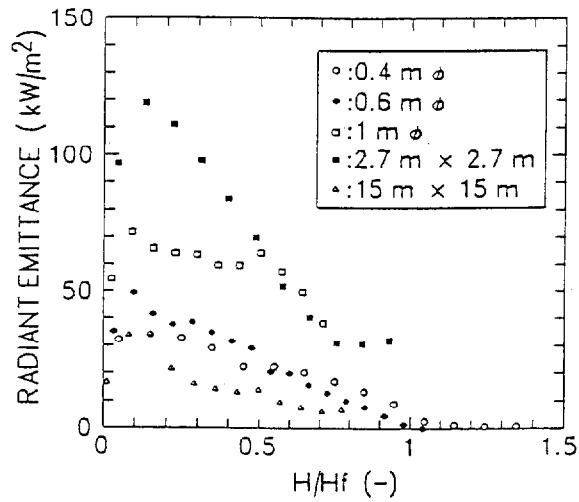


Figure 5 Local radiant emittance of several size crude oil fire

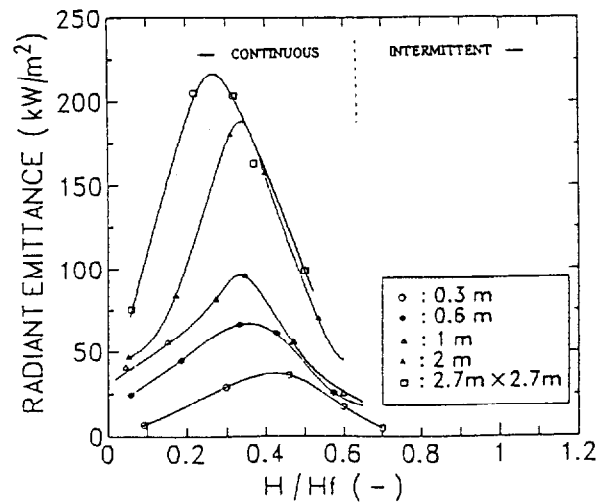


Figure 6 Local radiant emittance of several size heptane fire

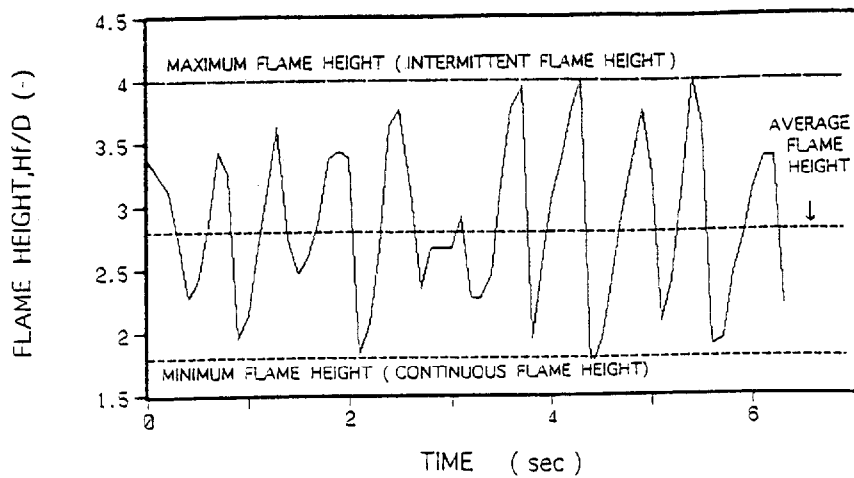


Figure 7 Pulsation of heptane 0.6m flame height
Flame height was decided using by IR-camera

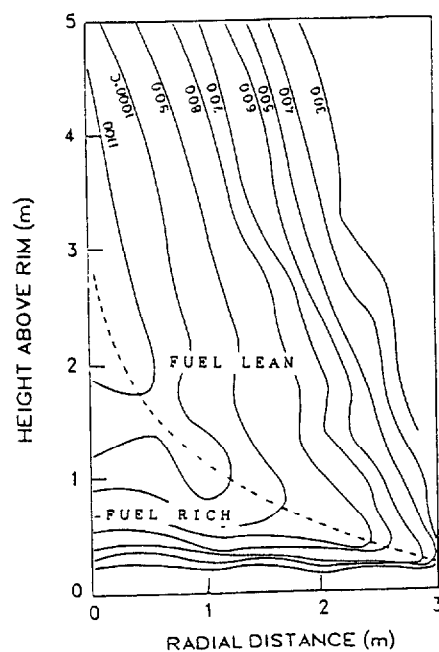


Figure 8 Isotherms of heptane 6 m flame
Temperature was measured by about 60 K-type thermocouples which diameter was 0.32 mm

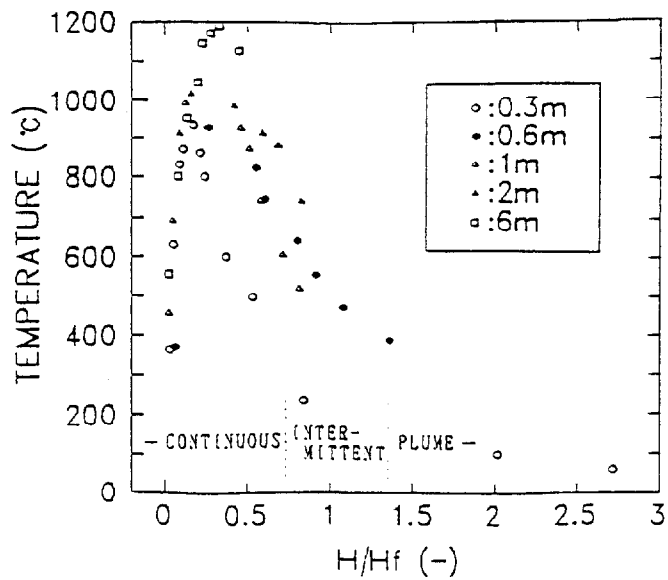


Figure 9 Temperature along several size heptane flame axis

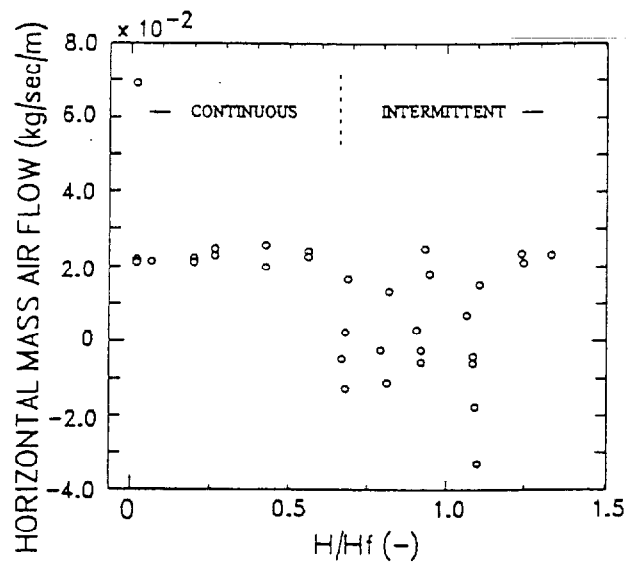


Figure 10 Horizontal mass air and gas flow in heptane 0.3 m fire measured by bi-directional tube

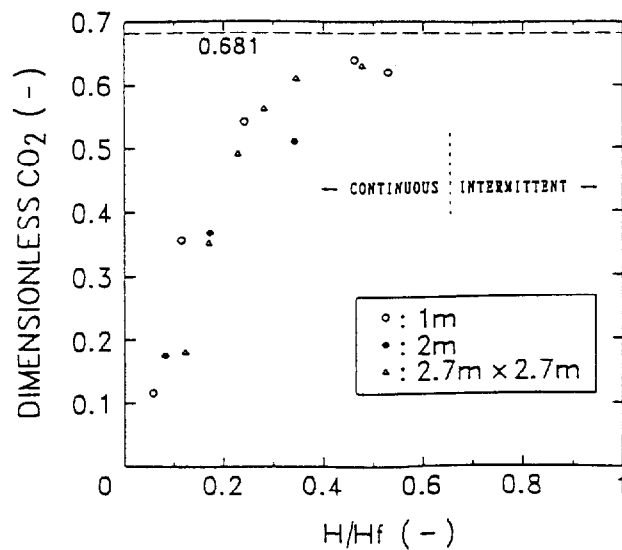


Figure 11 dimensionless CO_2^* along with flame axis measured with gas chromatograph

Discussion

Walter Jones: Would it be possible in this case to extend the work that's been done for smaller scale fires?

Hiroshi Koseki: Actually, the entrainment rate for the vertical direction has already been calculated and presented in another paper.

Patrick Pagni: This was very interesting in that there was an extreme in the radiation with the diameter. Our intuition from small scale is that radiation increases as the scale increases. How did you measure the radiant fraction?

Hiroshi Koseki: In this graph, the flames were sliced into small portions and in each portion, the radiation amount was calculated based upon temperature.